AN INVERSE ALGORITHM TO DETECT ELECTRICAL ACTIVITY OF THE BRAIN USING MEG

Qingxiang Li[(1)], and Om P. Gandhi[(2)]

[(1)]Department of Electrical and Computer Engineering, University of Utah, Rm. 3280, 50 South Central Campus Dr., Salt Lake City, UT84112, U.S.A. E-mail: eeqxl@eng.utah.edu

[(2)]As (1) above, but E-mail: gandhi@ece.utah.edu

ABSTRACT

In this paper, we have assumed two or four possible equivalent current dipoles (ECDs) in the two halves of the brain. A shaped model of the head represented by 6 mm voxels is used to calculate the forward magnetic fields at 74 locations of the MEG sensors. Tikhonov regularization and FOCUSS iteration are used to resolve the inverse problem. The algorithm is able to locate two or four sources at the same time. Typical error in magnitude of the current dipoles is less than ±5 percent, and the error in orientation is less than $\pm 4^{o}$ of angles ϑ and φ.

INTRODUCTION

Neural processes – perception, coordination, and cognition – are carried out via the propagation of electrical impulses from the brain. These impulses give rise to electromagnetic fields that can be measured extracranially by sensitive recording devices. The measurement of electric potentials over time referred to as EEG, and the measurement of magnetic signals as MEG. The practice through which we infer the inter-cranial sources that give rise to these measurements is termed the Neural Source Imaging problem, or inverse problem for EEG/MEG.

The inverse problem for MEG, also known as source localization for MEG is an active research area in bioelectromagnetics in recent years. Researchers are trying to locate and reconstruct the stimuli induced neural current sources, which are modeled as ECDs for many instances, (with varying amplitude, position and orientation in time) in the brain through the MEG recorded data, in order to understand the functioning of CNS and analyze the potential irregularity and several neurological diseases. The inverse problem is also a very challenging subject since it is a reconstruction problem for a 4-D profile (3-D in space and 1-D in time domain) in the presence of a relatively large measurement noise in practical MEG systems (typically 20-50% of the measured magnetic fields).

During the last 20 years, many inverse algorithms such as MUSIC, Beam-Forming, FOCUSS, etc, have been discussed to resolve the location, orientation, and magnitude of one to four ECDs in brain [1,2]. However, in previous research, a homogeneous sphere model of the head is mostly used for such inverse algorithms. Another model made up of a set of concentric spheres, each with homogeneous and isotropic conductivity, has also been used. An important aspect of inversion problem is to have realistic forward models such as those that have previously been developed for dosimetry of EM fields. Whereas the use of such a model for locating two ECDs over limited subvolumes of the brain (1.8×2.4×2.4 cm) has previously been described [3], we have extended the work for up to four ECDs that may be located over much larger subvolumes in the two halves of the brain. Our goal is to extend the search for the ECDs to the entire volume of the brain.

THE FORWARD MODEL

The forward model is the mathematical description of the mapping relationship between neural current sources in the brain and the external magnetic fields given by the lead field matrix **A** such that

$$\mathbf{A}\vec{J} = \vec{B}. \tag{1}$$

Where $\vec{B}$ is the MEG measurement data (which is corrupted by noise), and $\vec{J}$ is the source vector (first order sources), which is projected in x, y, and z directions. Because the neural sources are located inside the conductive media and are non-stationary, the induced currents caused as secondary sources will also make contribution to the external magnetic fields. In our study, we consider both first order and second order sources by means of 3-D impedance method [4]. The procedure to calculate the lead field matrix is as follows:

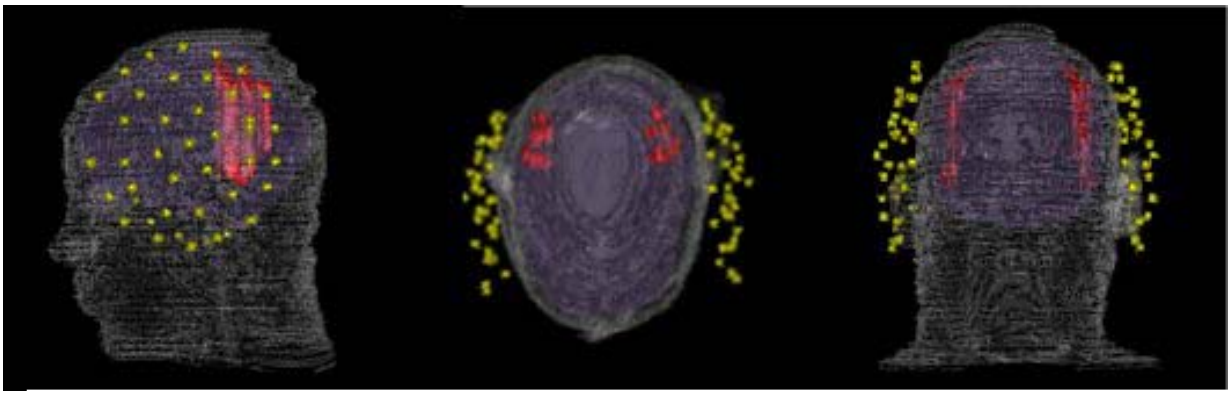

Fig. 1. Three visualizations of the human head model, and positions of sources and sensors. From left to right: The *y*-*z* plane, the *x*-*y* plane, and the *x*-*z* plane.

1. Use the Biot-Savart's Law to calculate the magnetic field distribution in air $\vec{B}'(r,t)$ caused by neural current sources.

$$\vec{B}'(\vec{r},t) = \frac{\mu_0 \vec{I}(t)}{4\pi} \oint \frac{dl(\vec{r}') \times (\vec{r} - \vec{r}')}{|\vec{r} - \vec{r}'|^3}. \tag{2}$$

2. Use the 3-D impedance method to calculate the induced currents inside the entire conducting volume of head model. In this method the whole model is represented by a 3-D network of impedances whose individual values are obtained from the complex conductivities for the various locations of the model. Using a quasi-static assumption that the phase of the incident electric and magnetic fields does not vary across the body being modeled, the impedances for various directions for the 3-D network can be written as

$$Z_m^{i,j,k} = \frac{\delta_m}{\delta_n \delta_p \sigma_m^{i,j,k}}. \tag{3}$$

Where *i, j, k* indicate the voxel index; *m* is the direction, which can be *x*, *y* and *z*, for which the impedance is calculated; $\sigma_m^{i,j,k}$ are the conductivities for the tissue in voxel *i*, *j*, *k*; δ_m is the thickness of the voxel in the *m*th direction; and δ_n and δ_p are the widths of the voxel in directions at right angles to the *m*th direction. With the use of the anatomically based model of the human head the induced current densities can then be calculated for each of the voxels.

3. From the induced currents thus calculated for the entire volume of the head, the external magnetic fields $\vec{B}(r,t)$ at the 74 sensor locations then can be calculated using Biot-Savart's law.

As given in [5], the heterogeneous anatomically-based human model was obtained from MRI scans of an adult male volunteer and has been segmented into 31 tissue types, 15 of which are associated with the region representing the head and neck. The anatomically-based model is resolved into pixels of dimensions 1.974×1.974 mm for the cross sectional cuts and thickness 3.0 mm along the vertical *z*-axis. For the present calculations, the voxel size is assumed to be 2.0×2.0×3.0 mm and 18 voxels are combined into one voxel of dimension 6.0×6.0×6.0 mm along the three axes, respectively. Three orthogonal views of the head model and the assumed sensor locations are shown in Fig. 1.

Fig. 2 shows comparison of the magnetic fields at the various sensor locations. It is shown that the external magnetic fields are altered greatly if secondary currents due to the conductivity of the tissues are ignored (such as for the air model), but are affected very little by using a shaped but homogeneous model rather that the detailed heterogeneous model. This obviates the need for modeling the patient-specific anatomic details as long as the shape of the head is properly modeled.

THE INVERSE ALGORITHM

The inverse problem of MEG is an ill-posed and under-determined problem. In a strict mathematical sense we are not able to solve an ill-posed and under-determined problem and get the correct solution. However using a priori knowledge we are able to get an answer that, hopefully, is close to the correct solution. One of the tools in this category is regularization which is used to tame the solution and keep it within reasonable limits, and one of the best known regularization methods is Tikhonov regularization which minimizes a linear combination of $\| \mathbf{A}\vec{J} - \vec{B} \|_2^2$ and $\| \mathbf{L}\vec{J} \|_2^2$, i.e.,

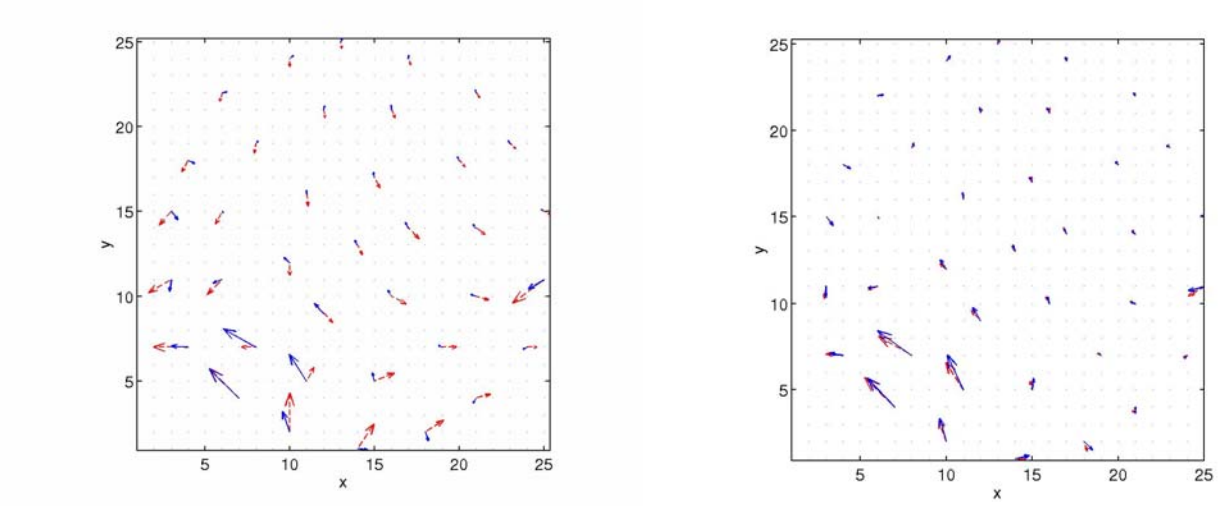

(a) (b)

Fig. 2. Comparison of magnetic field distribution at sensor positions. (a) Solid (blue) lines: magnetic fields calculated from air model, dashed (red) lines: magnetic fields calculated from heterogeneous model. (b) Solid (blue) lines: magnetic fields calculated from head-shaped homogeneous model, dashed (red) lines: magnetic fields calculated from heterogeneous model.

$$\vec{J} = \min_{\vec{J}}(\| \mathbf{A}\vec{J} - \vec{B} \|_2^2 + \alpha \| \mathbf{L}\vec{J} \|_2^2). \tag{3}$$

Where α is a parameter which controls the degree of regularization. A popular method of choosing the regularization parameter is to search through a range of values. The stopping criterion is determined by the trade-off curve between the solution norm that we minimize and the residual between actual data and the one predicted by the solution. The curve closely resembles an L-shape. The optimal parameter is located in the "corner" of this curve, where the solution norm that we minimize levels off while the residual norm remains small. The operator **L** introduces a "penalty" if $\vec{J}$ behaves undesirably. The simple choice is to let **L** be the identity and thereby the regularization restricts the norm of $\vec{J}$. In order to obtain a more focused solution, we implement an iterative procedure: FOCUSS [2] that modifies the **A** matrix using the estimate of the solution obtained at the previous step, to lower the effect of spurious solutions. In the iteration,

$$\mathbf{A}_k = \mathbf{A}_{k-1} \cdot \mathbf{W}_k. \tag{4}$$

Where $\mathbf{W}_k$ matrices are dimensionless scaling factors, which can be constructed by taking the diagonal elements to be the previous iterative step solutions,

$$\mathbf{W}_k = \begin{bmatrix} J_{1,k-1} & & 0 \\ & \ddots & \\ 0 & & J_{n,k-1} \end{bmatrix}. \tag{5}$$

Here $J_{i,k-1}$ represents the ith element of the vector $\vec{J}$ at the k-1 iteration, and k is the index of the iteration step.
This algorithm has been shown to always converge to a localized solution with no more than n non-zero elements, which is the number of measurements, with at least a quadratic rate of convergence. We take the norm $D = \| \vec{J}_k - \vec{J}_{k-1} \|$ as the iteration parameter, and stop the iteration when D less than some small number such as 0.5. We then use weighting functions to calculate the geometrical center of the solutions and thus obtain the source locations.
After the locations of sources are identified, we use the pseudo-inverse of matrix **A** to calculate the orientations and magnitudes based on the obtained locations of sources.

SIMULATION RESULTS

In this study, we have postulated that two or four dipole sources are located arbitrarily in the two halves of the brain over subvolumes of dimensions 1.8×3.0×6.0 cm represented by 100 voxels each (Fig. 1). We further assume that the depth of the individual sources may vary from 3.0 to 4.8 cm from the surface of scalp. It is recognized that the measured MEG signals may be corrupted by white Gaussian noise. Noise levels with signal to noise ratio (SNR) of 2 are added to the signals for each of the 74 magnetic field sensors which are distributed equally between the two sides of the head. A total of 200 repeated measurements are averaged in 12 to 24 blocks of 80 data to improve the SNR and inverse solutions.

In Table 1 we give some of the source locations selected for the inverse algorithm. If the source location is accurately detected as a result of the inversion algorithm, it is marked by √. Other than six out of 32 positions, the source locations are correctly detected. Even for the six positions, the error in the location of the source is generally no more than one voxel. In order to improve the accuracy even further we intend to interpolate the measured MEG data from the 74 measurement sensors to many additional intermediate sites (perhaps a total of 100 - 200 sites for each side of the brain). The algorithm is able to locate two or four sources at the same time. Typically, error in magnitude of the current dipoles is less than ±5 percent, and the orientation error is less than $\pm 4^{o}$ of angles ϑ and φ.
We are presently extending the algorithm so that the search will cover the whole brain or a substantial part thereof.

CONCLUSIONS

Non-invasive imaging techniques using the measured MEG data have been used to determine the location, orientation, and magnitude of several ECDs that are excited in the cerebral cortex in response to various stimuli or for memory or cognition. In this paper, we have used a head-shaped model to calculate the forward lead field matrix. The locations, orientations, and magnitudes of two or four ECD sources are successfully identified using the inverse algorithm which is a combination of Tikhonov regularization, FOCUSS iteration, and pseudo-inverse of matrix.

ACKNOWLEDGEMENT

The authors have greatly benefited from many helpful discussions with Professor Nagarajan of the University of Utah.

REFERENCES

[1] J.C. Mosher, R.M. Leahy, and P.S. Lewis, "EEG and MEG: Forward solutions for inverse methods," *IEEE Trans. Biomed Eng*, vol. 46, no.3, pp. 245-259, 1999.

[2] I.F. Gorodinitsky, J.S. George, and B.D. Rao, "Neuromagnetic source imaging with FOCUSS: a recursive weighted minimum norm algorithm," *Clinical Neurophysiology*, vol. 95, pp. 231-251, 1995.

[3] F. Borelli, O.P. Gandhi and G. D'Inzeo, "An electromagnetic inversion algorithm to detect neural activity using MEG," pp. 55-56, papers presented at the Twenty-third Annual Meeting of Bioelectromagnetics Society, St. Paul, MN June 10-14, 2001.

[4] N. Orcutt and O.P. Gandhi, "A 3-D impedance method to calculate power deposition in biological bodies subjected to time-varying magnetic fields," *IEEE Trans. BME*, vol. 35, pp. 577-583, 1988.

[5] O.P. Gandhi, "Some numerical methods for dosimetry: ELF to microwave frequencies," Radio Science, vol. 30, pp. 161-177, 1995.

Table 1. Comparison of assumed and estimated positions

Case Number	Assumed Source Position Coordinates (i,j,k)	Estimated Source Position Coordinates (i,j,k)	Position Error (i,j,k)	Case Number	Assumed Source Position Coordinates (i,j,k)	Estimated Source Position Coordinates (i,j,k)	Position Error (i,j,k)
1	(12,20,17)	√	0	5	(15,20,17)	√	0
	(15,21,17)	√	0		(12,24,21)	√	0
	(30,20,19)	√	0		(29,22,17)	√	0
	(27,21,17)	√	0		(27,24,21)	√	0
2	(12,20,19)	√	0	6	(13,20,18)	(13,20,19)	(0,0,1)
	(15,23,21)	√	0		(15,21,21)	√	0
	(27,20,19)	√	0		(29,20,19)	√	0
	(27,23,20)	(27,24,20)	(0,1,0)		(28,24,20)	√	0
3	(12,20,18)	√	0	7	(12,20,20)	√	0
	(15,24,17)	√	0		(15,21,18)	(15,22,17)	(0,1,-1)
	(30,20,18)	√	0		(30,20,20)	√	1
	(28,24,17)	(29,24,17)	(1,0,0)		(27,24,21)	√	0
4	(13,20,21)	√	0	8	(14,20,17)	√	0
	(14,21,17)	√	0		(15,21,21)	√	0
	(30,21,17)	(30,21,18)	(0,0,1)		(29,20,17)	√	0
	(27,21,21)	√	0		(27,21,21)	(28,21,21)	(1,0,0)

√ denotes a correct localization of the ECD from the inverse algorithm.